

# Coherent optical reflectance from a monolayer of large particles adsorbed on a glass surface

Mary Carmen Peña-Gomar, Francisco Castillo, Augusto García-Valenzuela, Rubén G. Barrera, and Elías Pérez

We develop a coherent-scattering model for the reflection of light from a monolayer of large particles and low surface coverage. The model takes into account multiple scattering between particles of the monolayer and with the substrate, and it can be used around the critical angle in an internal reflection configuration. We compare the results of the model with our own reflectivity data taken with latex particles adsorbed on a glass–water interface and with a simpler effective-medium model. © 2006 Optical Society of America

OCIS codes: 290.5850, 290.4210, 030.1670, 240.0310.

## 1. Introduction

Several papers have been published in the past years related to the optical reflectance of a monolayer of small particles adsorbed on a flat interface. When particles are very small compared to the wavelength, the particles may be treated in the dipole (or higher multipoles) approximation, and an effective-medium approach may be appropriate.<sup>1,2</sup> However, when particles are not small, light is scattered away from the specular direction and one may split the reflected optical fields in a diffuse component and a coherent component. The coherent component corresponds to the average of the optical fields and remains in the specular direction, whereas the diffuse component is related to the fluctuation of the optical fields from its average and is distributed over a wide range of reflection angles.<sup>3</sup> In experiments it is not difficult to extract the coherent component from the whole scat-

tered light. In this case one sometimes refers to the coherent reflectance of a well collimated beam of light as the reflectivity. It is also not difficult to measure the diffuse component of the scattered light. When particles are large, the effective-medium approach may no longer be valid and a scattering theory approach should be pursued.<sup>4</sup> By large particles we mean particles with radii such that the size parameter,  $(2\pi/\lambda) a$ , is comparable to or larger than 1. Here  $a$  is the particle radius and  $\lambda$  is the wavelength of radiation.

There are previous experimental studies on the adsorption of electrically charged latex particles on a flat surface based on measurements of the reflectance of TM (transverse magnetic or “*p*”) polarized light around the Brewster angle, defined by the refractive index of the substrate (glass) and of the continuous medium (water) where particles were suspended. The reflectance of TM polarized light at this angle is no longer zero when particles are adsorbed, and the minimum of the reflectance curve increases and slightly shifts to other angles.<sup>5–8</sup> In these works it was shown that by fitting a theoretical model to the experimental curves it was possible to retrieve accurately some physical properties of the adsorbed particles and the kinetics of adsorption. On the other hand, in Ref. 9 it was shown that the reflectance of a laser beam near the critical angle, in an internal-reflection configuration of a glass–water interface, changed strongly when electrically charged latex particles were adsorbed on the glass surface. The sensitivity of these measurements to the presence of the adsorbed colloidal particles was found to be much larger than when measuring the reflectance of TM

---

M. C. Peña-Gomar is with Facultad de Ciencias Físico-Matemáticas de la Universidad Michoacana de San Nicolás de Hidalgo, Edificio B, Ciudad Universitaria, CP. 58030, Morelia, Michoacán, México. F. Castillo and E. Pérez are with Instituto de Física, Universidad Autónoma de San Luis Potusí, Alvaro Obregón 64, 78000 San Luis Potusí, SLP, México. A. García-Valenzuela (garciaa@aleph.cinstrum.unam.mx) is with Centro de Ciencias Aplicadas y Desarrollo Tecnológico, Universidad Nacional Autónoma de México, Ciudad Universitaria, A.P. 70-168, México D.F. 04510, México. R. G. Barrera is with Instituto de Física, Universidad Nacional Autónoma de México, Apartado Postal 20-364, 01000 México D.F., México.

Received 19 April 2005; accepted 21 May 2005.

0003-6935/06/040626-07\$15.00/0

© 2006 Optical Society of America

polarized light close to the Brewster angle. This showed the potentiality of the internal-reflection experimental configuration as a sensitive tool to study the kinetics of the adsorption process, and to determine also the optical parameters of the adsorbed particles. The purpose of our work here is to perform these types of experiments and to develop a reliable theoretical model for the quantitative interpretation of the experimental results.

A simple theoretical model for the reflectance of light from a monolayer of large particles adsorbed on glass surface was proposed already in Refs. 5 and 6. The model takes into account the Mie scattering from the spherical particles and it is suitable for particles with large radii. Basically, the model in Refs. 5 and 6 approximates the coherent reflected wave as the superposition of the coherent reflected wave from an isolated monolayer and the reflected wave from the clean glass interface. It does not take into account, for example, the multiple reflections between the monolayer and the glass interface. Therefore the model is valid only for TM polarization near the Brewster angle since only then the reflection coefficient of the clean glass interface is practically null. Also in this model the coherent reflection amplitude from the isolated monolayer is calculated in the single-scattering approximation, which is valid only for small angles of incidence and low surface coverage (on the order of a few percent or less, depending on the particle's size and refractive index). In Ref. 5 the validity of the model for latex particles of refractive index 1.591 and for angles of incidence around the Brewster angle was checked against exact numerical calculations of the full electromagnetic problem. It was found that, although differences between the exact calculations and the approximate model could be large in some cases, estimating the particle size from fitting the approximate model to the experimental data gave accurate results for low values of the surface coverage and the particle's radii of up to about 1000 nm. Although exact numerical calculations are possible, considering the time these elaborate calculations take, it is necessary in practice to have an approximate model to implement a fitting routine for experimental data analysis. For experiments in an internal-reflection configuration and near the critical angle, the reflection coefficient of the clean glass interface is not small and the single-scattering approximation of the coherent reflection from the monolayer is not valid. Thus, to have an approximate model in these experiments; it is necessary to introduce multiple-scattering effects within the monolayer and with the glass interface.

One of the objectives of this work is to include these multiple-scattering effects by extending the model proposed in Refs. 5 and 6 to the treatment of the reflection of light from a monolayer of particles adsorbed on a glass-water interface, in an internal-reflection configuration. We will limit ourselves to monodisperse systems of spheres, all with the same refractive index. We will refer to our model as the "coherent-scattering model."

The paper is organized as follows: In Section 2 we

derive in the single-scattering approximation the coherent reflection from a monolayer of spherical particles. Then we improve this approximation by taking partially into account multiple scattering between particles within the monolayer, and construct the compound reflection coefficient that accounts for multiple reflections between the glass interface and the monolayer. We also take into account corrections to the reflectance due to the finite collimation of the incident optical beam. In Section 3 we compare the coherent-scattering model with the results of our own measurements. In Section 4 we compare the results of the coherent-scattering model with the ones obtained with an effective-medium model. Finally, in Section 5 we present our conclusions.

## 2. Theory

In Ref. 4 the coherent reflection and transmission of light from a dilute ensemble of identical spherical particles of radius  $a$ , whose centers are located at random within a slab of width  $d$ , was addressed. The geometry considered is shown here in Fig. 1(a). An incident plane wave,  $E_0 \exp(i\mathbf{k}^i \cdot \mathbf{r})\hat{\mathbf{e}}_i$ , is assumed. The coherent scattered waves to the right and to the left of the slab are plane waves,  $E_s^+ \exp(i\mathbf{k}^s \cdot \mathbf{r})\hat{\mathbf{e}}_s$ , and  $E_s^- \exp(i\mathbf{k}^r \cdot \mathbf{r})\hat{\mathbf{e}}_r$ , respectively. In the single-scattering approximation, and ignoring any correlation in the position of particles, the amplitudes  $E_s^+$  and  $E_s^-$  were found to be given by

$$E_s^+ = -E_0 \frac{\alpha}{\cos \theta_i} S(0), \quad (1)$$

$$E_s^- = -E_0 \frac{\alpha}{\cos \theta_i} \frac{\sin(k_z^i d)}{dk_z^i} S_n(\pi - 2\theta_i), \quad (2)$$

where  $\alpha = kd(3f/2x^3)$ ,  $n$  is 1 or 2 for TE or TM polarization, respectively,  $S_1(\theta)$  and  $S_2(\theta)$  are the non-zero elements of the amplitude scattering matrix,<sup>10</sup>

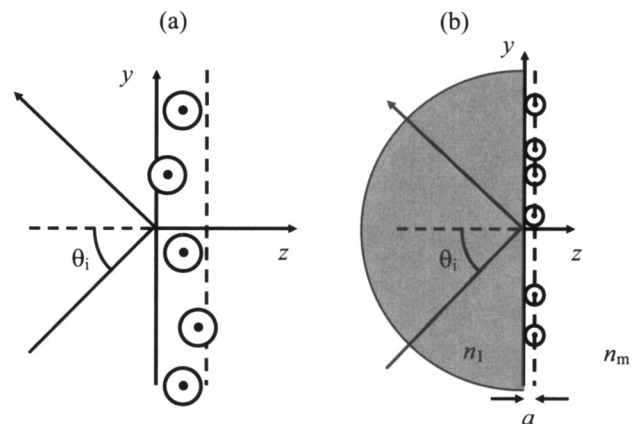


Fig. 1. (a) Geometry considered in the coherent reflection and transmission of a plane wave from a thin slab of a dilute random system of spherical particles; (b) geometry of the internal reflection configuration for reflectivity measurements from an adsorbed fractional monolayer of particles.

$S_1(\theta = 0) = S_2(\theta = 0) \equiv S(0)$ ,  $f$  is the volume fraction occupied by the spheres,  $\theta_i$  is the angle of incidence,  $k_z^i = k \cos \theta_i$ ,  $k$  is the wavenumber in the medium surrounding the spheres, which we will call the “matrix” medium, and  $x = ka$ , where  $a$  is the radius of the particles. The coherent reflection and transmission coefficients from a slab of randomly placed particles of thickness  $d \ll 1/k$  follow from these expressions:

$$t_s = 1 - \frac{\alpha}{\cos \theta_i} S(0), \quad (3)$$

$$r_s = -\frac{\alpha}{\cos \theta_i} S_n(\pi - 2\theta_i), \quad (4)$$

The derivation leading to Eqs. (3) and (4) assumes that the center of the spheres is contained within a slab between  $z = 0$  and  $z = d$ . This means that half a sphere may lay outside the slab from either side. We can obtain the reflection and transmission coefficients of the coherent wave from a monolayer of particles from the previous expressions in the following manner. Consider  $N$  particles inside a slab of volume  $Ad$ , where  $A$  is the area of the slab in the  $x$ - $y$  plane and  $d$  is the thickness of the slab along the  $z$  axis, recalling that  $f = (N/V)(4/3)\pi a^3$ , we have that

$$\alpha \equiv \frac{3}{2} \frac{f}{x^3} kd = \frac{2\Theta}{x^2},$$

where  $\Theta = (N/A)\pi a^2$ . Since the right-hand side of the equation does not depend on  $d$ , we can take the limits  $d \rightarrow 0$  and  $N, A \rightarrow \infty$  while keeping the surface number density  $N/A \equiv \rho_s$  constant. In this limit,  $\Theta$  is the surface coverage and the plane passing through the center of all the particles contained in the (partially covered) monolayer is the plane  $z = 0$ . This may be called the plane of the monolayer.

Now, we propose an approximation that includes, in an average way, multiple-scattering effects among the particles, by considering that the field driving the scattering process is the transmitted wave rather than the incident one. Then we can write

$$t_s E^i = E^i - \frac{\alpha S(0)}{\cos \theta_i} t_s E^i, \quad (5)$$

$$r_s E^i = -\frac{\alpha S_n(\pi - 2\theta_i)}{\cos \theta_i} t_s E^i. \quad (6)$$

Solving this pair of equations we obtain the following transmission and reflection coefficients for the coherent wave:

$$t_s = \frac{\cos \theta_i}{\cos \theta_i + \alpha S(0)}, \quad (7)$$

$$r_s = -\frac{\alpha S_n(\pi - 2\theta_i)}{\cos \theta_i + \alpha S(0)}. \quad (8)$$

Note that these coefficients behave correctly at grazing incidence. Therefore, as long as the surface coverage of the spheres is small, that is,  $\Theta \ll 1$ , one can expect that the previous formulas provide a good approximation at any angle of incidence, including grazing incidence. Now, if we assume that the plane of the monolayer is at  $z = z_0$ , then the reflection coefficient is multiplied by the phase factor  $\exp(2ik_z^i z_0)$ .

Let us now consider the case of interest in this paper, where the base of a glass prism of index of refraction  $n_1$  coincides with the plane  $z = 0$  and is immersed in a matrix of index of refraction  $n_m$ . Then let us suppose that a monolayer of spherical particles of radius  $a$  is adsorbed on the base of the prism, as depicted in Fig. 1(b). The plane of the monolayer, as defined above, is now at  $z = a$ . If a plane wave is now incident from the prism side to the interface at an angle  $\theta_i$  (from the normal), a plane wave will be transmitted outside the prism into the matrix, making an angle  $\theta_m$ . Both angles are related through Snell’s law,  $n_1 \sin \theta_i = n_m \sin \theta_m$ . The transmitted wave is reflected back and forth between the monolayer and the base of the prism; thus the reflected coherent wave from the base of the prism contains the superposition of all the coherent waves reflected from the monolayer and transmitted back into the prism. This is analogous to the multiple reflections within a homogeneous slab between two homogeneous mediums. The resulting compound reflection coefficient for the coherent wave is given by

$$r_{CSM} = \frac{r_{12}(\theta_i) + r_s(\theta_m)}{1 + r_{12}(\theta_i)r_s(\theta_m)}, \quad (9)$$

where  $r_{12}$  is the Fresnel reflection coefficient between the prism and the matrix medium without particles, and  $r_s$  is given by

$$r_s(\theta_m) = -\frac{\alpha S_n(\pi - 2\theta_m)}{\cos \theta_m + \alpha S(0)} \exp(2ik_z^m a), \quad (10)$$

with  $k_z^m = k_0 n_m \cos \theta_m = k_0 \sqrt{n_m^2 - n_1^2 \sin^2 \theta_m}$ ,  $S(0)$  and  $S_n(\pi - 2\theta_m)$  are evaluated for the particles surrounded by the liquid of index of refraction  $n_m$ , and  $\theta_m = \sin^{-1}[(n_1/n_m) \sin \theta_i]$ . Thus Eq. (9) is the plane-wave reflection coefficient for the prism–liquid interface when a fraction of a monolayer is adsorbed on it, at the liquid interface. When the angle of incidence is larger than the critical angle of the prism–matrix interface,  $\theta_c = \sin^{-1}(n_1/n_m)$ ,  $\theta_m$  becomes complex. Therefore the average field exciting the particles is actually an evanescent wave. This poses no problem in our formulation in terms of the elements of the amplitude scattering matrix because the mathematical procedure remains valid for an exciting field with a complex wave vector.

However, in the experiment one is not using a plane wave. Instead one uses a well-collimated beam. Most laser beams have a Gaussian intensity profile. The reflectance of a Gaussian beam can be calculated

from the plane-wave reflection coefficient,  $r$ , as<sup>11</sup>

$$R(\theta_i) = \frac{\omega_0 k_1}{\sqrt{2\pi}} \int_0^{\pi/2} |r(\theta)|^2 \exp\left[-\frac{(\omega_0 k_1)^2}{2} (\theta - \theta_i)^2\right] d\theta, \quad (11)$$

where  $\omega_0$  is the beam's waist radius and  $k_1$  is the wavenumber of light in the incident medium (in this case the prism). For well-collimated beams, the limits of this integral can be extended to  $\pm\infty$  with negligible errors. The effect of a finite  $\omega_0$  is stronger where the derivative of  $|r(\theta)|^2$  is largest. In general, this is near the critical angle between the prism and the external medium. In our experiments a semicylindrical prism is used. The laser beam is focused upon the entrance to the prism due to the curvature of its surface. Then the cross section of the laser beam actually becomes elliptical. The value of  $\omega_0$  that should be used with Eq. (11) is the semiaxis of the ellipse along the plane of incidence. From geometrical considerations we may approximate  $\omega_0$  inside the prism as  $\sim \lambda n_1 Y / \pi \omega_0^{\text{out}}$ , where  $Y$  is the radius of the semicylindrical prism and  $\omega_0^{\text{out}}$  is radius of the beam outside the prism. In our experiments  $\omega_0$  is smaller than  $\omega_0^{\text{out}}$ , which means that the laser beam is less collimated, thus using Eq. (11) to calculate accurately the reflectance becomes essential.

### 3. Measurements

To test our model against experimental data we measured the coherent reflectance of a laser beam, at different angles of incidence, from the base of a semicylindrical prism with a monolayer of latex particles adsorbed onto it. Our experimental setup is shown in Fig. 2. The half-cylinder prism ( $n_1 = 1.51$ ) is inserted laterally on the cylindrical container and mounted on top of a high-precision goniometer to measure and control the angle of incidence. A linearly polarized He-Ne laser beam ( $\lambda = 0.6328 \mu\text{m}$ ) of Gaussian cross section with a diameter of approximately 0.81 mm is reflected from the base of the prism. Then the angle of incidence is adjusted by rotating the goniometer, and the reflected optical power is collected by a silicon photodetector and a digital voltmeter. First, the container was filled with de-ionized water and a plot of the reflectance as a function of the angle of incidence about the critical angle,  $\theta_c = \sin^{-1}(n_m/n_1)$ , was registered. This curve was used to adjust the value of  $\omega_0$  and correct any systematic error in the angle of incidence  $\theta_i$ . Then the water was replaced by a dilute colloidal suspension of electrically charged latex particles. The particles adsorbed gradually over time on the base of the prism. After approximately 10–15 min, the colloidal suspension was replaced by de-ionized water, stopping the adsorption process. A second reflectance plot over the same angular range as the previous one for water was registered. The contribution of diffuse light to the reflectivity signal was checked to be negligible. After each experiment the prism was dismantled from the container and its

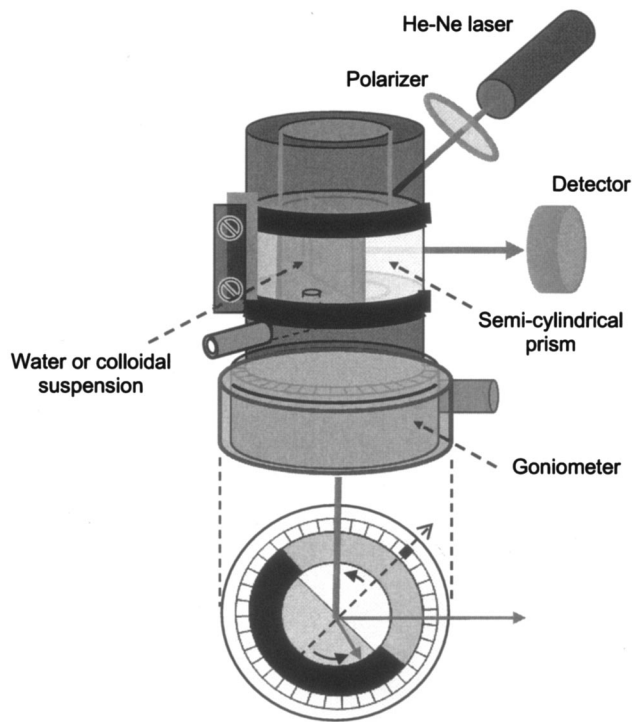


Fig. 2. Schematic of the experimental setup.

base was inspected with an optical microscope to ensure that a monolayer had been formed.

In Figs. 3(a)–3(c) we show plots of the measurements of the reflectivity as a function of the angle of incidence around the critical angle for both a clean prism surface in water and after the monolayer of particles had been adsorbed. The particle sizes in the experiments corresponding to Figs. 3(a), 3(b), and 3(c) were 137, 256, and 344 nm, respectively. In these figures we also show micrographs taken from the base of the prism after the experiments. An estimation of the surface coverage from the micrographs proved to be unreliable. The reason is that an unknown amount of particles was desorbed from the prism surface when exposed to air while the prism was taken to the optical microscope. Therefore, to compare theory with experiment, we left  $\Theta$  as an adjustable parameter. In the figures we also plot a reflectance curve calculated with our coherent-scattering model. The refractive indices used for the prism, for water, and for the particles are 1.515, 1.331, and 1.59, respectively. Also, for the three graphs in Fig. 3 we used  $\omega_0 = 18.6 \mu\text{m}$  and  $\lambda = 0.6328 \mu\text{m}$ . The value of  $\Theta$  was adjusted to best fit the experimental data. We see in the figures that the theoretical curves reproduce fairly well the experimental data, although some discrepancies between theory and experiment can be appreciated. These discrepancies may be due to the formation of particle aggregates on the surface that are not accounted for in the model. The formation of aggregates on the prism surface can be appreciated in the micrographs taken after the optical measurements.

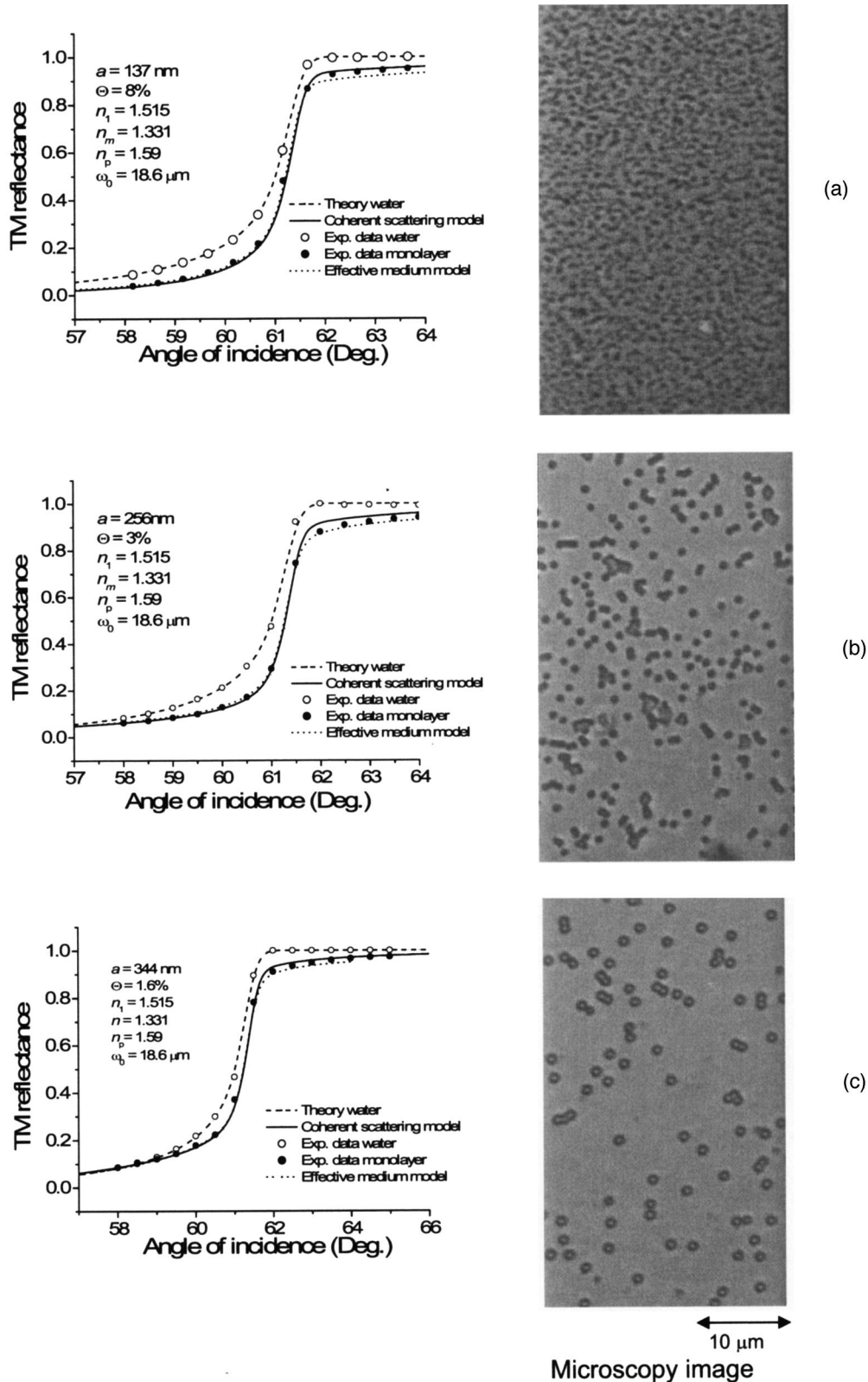


Fig. 3. Experimental data of the reflectance of a TM polarized He–Ne laser beam from a clean glass–water interface (open circles) and with an adsorbed monolayer of latex particles (full circles). The radii of the particles are (a) 137, (b) 256, (c) 344 nm. The refractive index of the glass, water, and particles is 1.515, 1.331, and 1.59, respectively. Theoretical curves with the coherent-scattering model (full curve) and with the effective-medium model (dotted curve) are also plotted. The values of the surface coverage used to adjust the scattering-theory model to the experimental data are (a) 0.08, (b) 0.03, and (c) 0.016. Microscopic images from the base of the prism after the experiments are also shown.

#### 4. Comparison with an Effective-Medium Model

It is instructive to compare the results for the reflectance obtained with the coherent-scattering model with the one obtained with an effective-medium model. Effective-medium models (EMM) have been used for monolayers of particles on a flat substrate when particles are small compared to the wavelength of radiation;<sup>1,2,8</sup> however, there have been attempts to use them when particles are not small (see, for example, Ref. 12). We may think of replacing the random monolayer of particles by an artificial film with effective properties. A simple model may be to consider a film of thickness equal to the diameter of the particles,  $2a$ , and an effective refractive index. In a *bulk*, dilute colloidal system and when the colloidal particles are not necessarily small with respect to the wavelength of the incident beam, a well-validated effective index of refraction is the one first derived by van de Hulst,<sup>13</sup> and given by  $\tilde{n}_{eff} = n_m[1 + i\gamma S(0)]$ , where  $\gamma = 3f/2x^3$ .<sup>4,13</sup> We have added a tilde on top of  $n_{eff}$  just to remark that it is a complex quantity. In the case of a monolayer one might (daringly) assume that the effective index of refraction is the same as in the bulk, thus one should simply replace in the expression for  $n_{eff}$  the volume fraction of particles  $f$  in the effective film by  $(2/3)\Theta$ , where  $\Theta$  is the surface coverage. Therefore the reflectance in this effective-medium model is calculated using the well-known expression for reflection coefficient in a three-layered media,

$$r_{EMM} = \frac{r_{12} + r_{23} \exp(2ik_{z2}d)}{1 + r_{12}r_{23} \exp(2ik_{z2}d)}. \quad (12)$$

Here  $r_{12}$  and  $r_{23}$  are the Fresnel reflection coefficients for the glass–film interface and the film–water interface, respectively,  $k_{z2} = k_0(\tilde{n}_{eff}^2 - n^2 \sin^2 \theta_i)^{1/2}$ , and  $d = 2a$ . Evaluation of the Fresnel reflection coefficients is done using the van de Hulst's effective refractive index,  $\tilde{n}_{eff}$ . In Figs. 3(a)–3(c) we also plot the reflectance curve predicted by the effective-medium model just described, assuming the same value of  $\Theta$  used to adjust the coherent-scattering model. We can see that the effective-medium model also reproduces the experimental data relatively well. The differences between the experimental data and the effective-medium model are similar to those with the coherent-scattering model, even though both models do not coincide exactly. For larger surface coverage, larger particle radii, or larger refractive-index contrast than those in our experiments, the reflectance curves around the critical angle predicted by the effective-medium model differ more noticeably from those predicted by the coherent-scattering model.

Also numerical evaluation of the reflectance using Eqs. (9) and (12) show that the coherent-scattering model and the effective-medium model predict quite different contributions of the colloidal particles to the reflectance at other angles of incidence. To illustrate this, we consider two examples: (i) Latex particles with refractive index  $n_p = 1.6$ , radius  $a = 350$  nm,

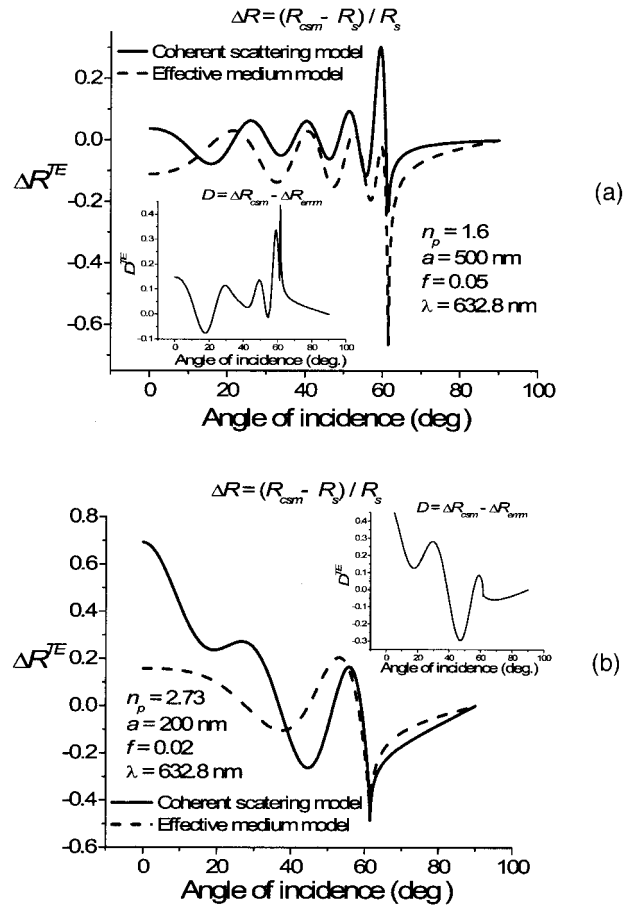


Fig. 4. Plots of the change in reflectance,  $\Delta R = (R_{\text{model}} - R_s)/R_s$ , of a glass–water interface (refractive indices 1.515 and 1.331, respectively) due to the adsorption of (a) latex and (b)  $\text{TiO}_2$  (rutile) particles of radii 500 and 200 nm, respectively. A wavelength of 632.8 nm was assumed. The surface coverage fraction was assumed to be (a) 5% and (b) 2%. The full curve is with the coherent-scattering model and the dashed curve is with the effective-medium model.

and assuming a surface coverage fraction  $\Theta = 0.05$  and (ii)  $\text{TiO}_2$  (rutile) particles with refractive index  $n_p = 2.73$ , radius  $a = 200$  nm, and assuming  $\Theta = 0.02$ . Both examples were considered in an internal reflection configuration with a glass–water interface and with TE (transverse electric or “s”) polarized light of wavelength  $\lambda = 632.8$  nm. In Fig. 4 we plot the relative difference in TE reflectance due to the adsorbed particles predicted by both models in  $\Delta R = (R_{\text{model}} - R_s)/R_s$ , where  $R_{\text{model}}$  is calculated with either the coherent-scattering or the effective-medium model, and  $R_s$  is the reflectance of the clean glass–water interface. It can be appreciated in Fig. 4 that both models predict quite different values of  $\Delta R$  at most angles of incidence. These differences increase for larger surface coverage. In the inset of the figures we plot the difference of  $\Delta R$  predicted by both models. For angles of incidence just before the critical angle of the glass–water interface, and for higher angles of incidence, the curves of  $\Delta R$  versus  $\theta_i$  have similar shapes although different magnitudes. This

was found to be true also for TM polarization. This means that the reflectance using the effective-medium model may be adjusted reasonably well to the reflectance predicted by the coherent-scattering model in an internal-reflection configuration and around the critical angle, but it would be necessary to use a smaller value of the surface coverage in the effective-medium model. Further experiments are necessary to see whether the coherent-scattering model remains accurate in these cases.

Even though the effective-medium model proposed here seems to predict consistently the reflectance curves around the critical angle for small enough surface coverage, we must point out its heuristic character. In particular, the thickness of the effective film was chosen to be  $2a$ , without a clear physical justification. We have checked that other choices of this "effective" thickness will weaken the accuracy of the effective film model around the critical angle, at least in the case of the experiments presented here. Therefore, in general, we could not advise with confidence the use of an effective film model to estimate the surface coverage factor, or any other parameter of the particles for that matter. At other angles of incidence the effective-medium model simply should not be used.

## 5. Conclusions

We developed a simple coherent-scattering model for light reflection from a monolayer of large particles adsorbed on a flat interface. The model is valid for all angles of incidence in an internal or external reflection configuration as long as the surface coverage is small compared to one. By large we mean particles with radii comparable to the wavelength of the incident radiation. We performed experimental measurements of the optical reflectance from a glass–water interface in an internal reflection configuration around the critical angle. Electrically charged latex particles were adsorbed on the glass–water interface, forming a monolayer with small values of the surface coverage. The coherent-scattering model could reproduce well the experimental data. Only the value of the surface coverage was adjusted to best fit the experimental curve.

Additionally, we compared the coherent-scattering theory model with an heuristic effective-medium model and found that, in general, they predict quite different contributions to the reflectance from the presence of an adsorbed monolayer of large particles. However, around the critical angle in an internal-reflection configuration, both models predict similar results at low enough values of the surface coverage. At other angles of incidence, and for large particles, the effective-medium model should not be used at all. For larger surface coverage more experiments are

necessary to check the predictions presented in this work.

We are grateful to Ma. Lourdes González-González and Asur Guadarrama-Santana for technical support. We also acknowledge financial support from Dirección General de Asuntos del Personal Académico from Universidad Nacional Autónoma de México through grants IN112905 and IN108402-3, PROMEP, Proyecto de Intercambio px-230 UNAM-UASLP, and Conacyt 36464-E. M.C. P.-G. acknowledges a fellowship from Consejo Nacional de Ciencia y Tecnología (México). The authors also thank J.L. Sánchez (UASLP) for Fig. 2.

## References

1. R. G. Barrera, M. Castillo-Mussot, G. Monsivais, P. Villaseñor, and W. L. Mochán, "Optical properties of two-dimensional disordered systems on a substrate," *Phys. Rev. B* **43**, 13819–13826 (1991).
2. C. Beitia, Y. Borensztein, R. Lazzari, J. Nieto, and R. G. Barrera, "Substrate-induced multipolar resonances in supported free-electron metal spheres," *Phys. Rev. B* **60**, 6018–6022 (1999).
3. E. M. Ortiz, F. González, J. M. Saiz, and F. Moreno, "Experimental measurements of the statistics of the scattered intensity from particles on surfaces," *Opt. Express* **10**, 190–195 (2002), <http://opticsexpress.org>
4. R. G. Barrera and A. García-Valenzuela, "Coherent reflectance in a system of random Mie scatterers and its relation to the effective-medium approach," *J. Opt. Soc. Am. A* **20**, 296–311 (2003).
5. E. A. van der Zeeuw, L. M. Sagis, G. J. M. Koper, E. K. Mann, M. T. Haarmans, and D. Bedeaux, "The suitability of angles scanning reflectometry for colloidal particle sizing," *J. Chem. Phys.* **105**, 1646–1653 (1996).
6. E. A. van der Zeeuw, L. M. C. Sagis, and G. J. M. Koper, "Direct observation of swelling of non-cross-linked latex particles by scanning angle reflectometry," *Macromolecules* **29**, 801–803 (1996).
7. D. Bedeaux and J. Vlieger, *Optical Properties of Surfaces* (Imperial College Press, 2004).
8. M. R. Böhmer, E. A. van der Zeeuw, and G. J. M. Koper, "Kinetics of particle adsorption in stagnation point flow studied by optical reflectometry," *J. Colloid Interface Sci.* **197**, 242–250 (1998).
9. M. Peña-Gomar, Ma. L. González-González, A. García-Valenzuela, J. Antó-Roca, and E. Pérez, "Monitoring particle adsorption by laser reflectometry near the critical angle," *Appl. Opt.* **43**, 5963–5970 (2004).
10. C. F. Bohren and D. R. Huffman, *Absorption and Scattering of Light by Small Particles* (J. Wiley 1983).
11. A. Garcia-Valenzuela, M. C. Peña-Gomar, and J. Villatoro, "Sensitivity analysis of angle-sensitive-detectors based on a film resonator," *Opt. Eng.* **42**, 1084–1092 (2003).
12. P. A. Ngankam, Ph. Lavalle, J. C. Voegel, L. Szyk, G. Decher, P. Schaaf, and F. J. G. Cuisinier, "Influence of polyelectrolyte multilayer films on calcium phosphate nucleation," *J. Am. Chem. Soc.* **122**, 8998–9005 (2000).
13. H. C. van de Hulst, *Light Scattering by Small Particles* (Wiley, 1957).